Chapter AM (Aeromagnetic Modeling)

AN INTERPRETATION OF PROPRIETARY AEROMAGNETIC DATA OVER THE NORTHERN ARCTIC NATIONAL WILDLIFE REFUGE AND ADJACENT AREAS, NORTHEASTERN ALASKA

by Jeffrey D. Phillips¹

in The Oil and Gas Resource Potential of the 1002 Area, Arctic National Wildlife Refuge, Alaska, by ANWR Assessment Team, U.S. Geological Survey Open-File Report 98-34.

1999

This report is preliminary and has not been reviewed for conformity with U.S. Geological Survey editorial standards (or with the North American Stratigraphic Code). Use of trade, product, or firm names is for descriptive purposes only and does not imply endorsement by the U.S. Geological Survey.

¹ U.S. Geological Survey, MS 964, Denver, CO 80225

TABLE OF CONTENTS

ABSTRACT
INTRODUCTION
DATA PREPARATION
DEPTH TO MAGNETIC BASEMENT
SEDIMENTARY MAGNETIC STRUCTURE AND STRATIGRAPHY
CONCLUSIONS
REFERENCES

FIGURES

- AM1. Index map showing limits of aeromagnetic coverage.
- AM2. Power spectra of the aeromagnetic data and of a model consisting of three equivalent magnetic layers.
- AM3. Bandpass filters corresponding to the three equivalent magnetic layers.
- AM4. Results of bandpass filtering displayed along a north-south profile.
- AM5. Lowpass magnetic field, showing magnetic anomalies produced largely within the Franklinian basement.
- AM6. Minimum depth to magnetic basement as estimated from the lowpass magnetic field.
- AM7. Maximum depth to magnetic basement as estimated from the lowpass magnetic field.
- AM8. Magnetic model for the combined highpass and bandpass magnetic field along seismic reflection profile 84-6.
- AM9. Magnetic model for the combined highpass and bandpass magnetic field along seismic reflection profile 85-22.
- AM10. Magnetic model for the combined highpass and bandpass magnetic field along seismic reflection profile 85-50.
- AM11. Near-surface fault map interpreted from the highpass aeromagnetic anomalies.

ABSTRACT

Highpass-filtered aeromagnetic data can be used to map shallow geologic structures, such as folds and faults, within the sedimentary units at the northern end of the Arctic National Wildlife Refuge (ANWR). Structural interpretations based on the aeromagnetic data are consistent with interpretations based on seismic reflection profiles, and provide important information about the location, size, and faulting of shallow petroleum prospects within the Thin-Skinned Thrust-Belt Play. Lowpass-filtered aeromagnetic data can be used to map the depth to the magnetic basement surface beneath the shallow sedimentary section. This surface can be compared to the Franklinian basement surface as interpreted from the seismic reflection data. Such comparisons yield information about the magnetic composition of units within the deeper parts of the Thin-Skinned Thrust Belt Play, and within deeper plays related to the Franklinian basement.

INTRODUCTION

The sedimentary basin within the 1002 area (Figure AM1) at the northern end of the Arctic National Wildlife Refuge (ANWR) is largely covered by tundra and surficial deposits, so most of our knowledge about the geology of the basin comes from wells adjacent to ANWR and from proprietary seismic reflection profiles collected within ANWR during 1984 and 1985 by a consortium of oil companies (Molenaar, 1987). From this sampling, we know that the basin consists exclusively of sedimentary rocks that are primarily of marine origin, and that it can be divided into a deformed zone containing thrust faults and folds in the south and an undeformed zone containing flat-lying beds in the north (Bird, Chap. GG). The youngest sedimentary units (Early Cretaceous through Quaternary in age) were derived from the Brooks Range to the south, and are called the "Brookian sequence" (Bird, Chap. GG; Bird and Molenaar, 1987).

The seismic reflection profiles are spaced about three miles apart. They contain no information about structure above sea level, and little information about structure above the base of the permafrost layer at about 1000 to 2000 feet (300 to 600 m) below the ground surface (Molenarr, 1987; Brewer, 1987; Foland and Lalla, 1987). Within the more intensely deformed parts of the basin the seismic data quality is poor; elsewhere it is good. Shot-hole paleontology samples, gravity measurements, and some ground-based magnetic profiling supplement the seismic data.

In preparation for the current assessment, the USGS acquired proprietary high-sensitivity aeromagnetic data from World Geoscience, Inc. These data were flown in 1991 and 1992 by BGM Airborne Surveys. Flight lines were spaced _ mile (800 m) apart and terrain clearance was 1000 feet (300 m) for most of the area (Figure AM1). Our licensing agreement prohibits us from publishing these data in map form at wavelengths shorter than 4 km.

DATA PREPARATION

The flight line aeromagnetic data were projected and gridded on a 200 m grid. The resulting map clearly showed both broad, high-amplitude anomalies related to magnetic sources within the basement, and narrow, linear, low-amplitude anomalies related to shallow structures within the sedimentary section. A matched filtering approach (Phillips, 1997) was used to separate these two sets of anomalies. Matched bandpass filters were designed by fitting a power spectrum based on simple magnetic layers to the power spectrum of the aeromagnetic data (Figure AM2). A bandpass filter corresponding to each layer (Figure AM3) was applied to the data in order to extract the magnetic anomalies associated with that layer. The separation of the narrow, linear anomalies from the broad high-amplitude anomalies was successful (Figure AM4).

DEPTH TO MAGNETIC BASEMENT

The lowpass aeromagnetic data (Figure AM5) appear to show magnetic anomalies produced largely within the Franklinean basement. These data were processed to estimate the depths to deep magnetic contacts using the horizontal gradient method (Roest and Pilkington, 1993; Phillips, 1997). Such depth estimates are model-dependant and define a "magnetic basement" surface, which may differ from the geologic basement surface if (1) the model used is over-simplified or inappropriate, or (2) the magnetic sources actually lie significantly below (or above) the geologic basement surface. The depths were first estimated assuming that the magnetic source bodies within the basement were very thick; this yielded minimum estimates for the depth to magnetic basement. Then the depths were re-estimated assuming that the magnetic source bodies were very thin; this yielded maximum estimates for the depth to magnetic basement. The two sets of depth estimates were gridded to form continuous magnetic basement surfaces (Figures AM6 and AM7). The two magnetic basement surfaces were compared to the Top of the Pre-Mississipian (TPM) surface as interpreted from the seismic data (Grow and others, Chap. NA). The minimum magnetic basement depths (Figure AM6) lie above the TPM

surface over most of the 1002 area; the magnetic basement drops below the TPM surface only in the extreme south and in the northwest. This implies that if most of the magnetic anomalies are produced at the TPM surface, then the source bodies are not extremely thick. The maximum depths to magnetic basement (Figure AM7) lie below the TPM surface over much of the 1002 area, with the exception of the Hula-Hula Low and the Demarcation Basin. This implies that if most of the magnetic anomalies are produced at the TPM surface, then the source bodies are not extremely thin. We conclude that, by appropriately varying the source thickness of our interpretative model, it should be possible to bring the magnetic depth estimates into agreement with the TPM surface over much of the 1002 area. Exceptions include the Hula-Hula Low and the Demarcation Basin, both of which appear to be masked by shallow magnetic sources (Figure AM7). Because we know that sedimentary magnetic sources exist within the basin (see below), it is reasonable to assume that the TPM has no magnetic signature in these two areas, and that the depth estimates are focusing on shallower sedimentary magnetic sources. Note that the seismic data cannot adequately define the TPM over the parts of the Demarcation Basin that are further than 6 km offshore; here the magnetic basement may actually be providing better estimates of the TPM depths. Additional areas where the magnetic basement and the TPM disagree include the extreme southern and northwestern areas where the magnetic sources are always deeper than the TPM (Figure AM6). Here it seems likely that the TPM has no magnetic signature, and the depth estimates are focusing on sub-basement magnetic sources. In areas where the deepest magnetic sources are always above the TPM, such as over the Hula-Hula Low and the near-shore parts of the Demarcation Basin, apparent structures seen in figures AM6 and AM7 could be interpreted as possible prospects within the deeper Thin-Skinned Thrust-Belt Play (Perry and others, Chap. P8).

SEDIMENTARY MAGNETIC STRUCTURE AND STRATIGRAPHY

Magnetic models were constructed along selected seismic reflection profiles, using the combined highpass and bandpass magnetic anomalies (Figures AM8, AM9, and AM10). In general it was possible to model the magnetic anomalies using dipping, folded, and faulted sedimentary magnetic layers within the Brookian sequence that conformed to the interpreted seismic sections (Potter and others, Chap. BD). The magnetized layers are generally Eocene and Paleocene in age. In order to reproduce the amplitudes and signs of the observed anomalies within the constraints of the geologic dips observed on the seismic sections, reversed remanent magnetizations were required in some layers of the models. Such magnetizations could be the

result of detrital magnetization acquired during deposition at times when the earth's magnetic field had reversed polarity (Phillips and others, in press).

The highpass aeromagnetic anomaly map (not shown due to proprietary restrictions) was interpreted to produce a near-surface fault map for the northern ANWR area (Figure AM11). The interpreted faults are based largely on apparent offsets and truncations of anomalies produced by magnetized sedimentary units. Some of the faults are evident in the seismic reflection data, and in structural interpretations based on the seismic reflection network and surface geology (Potter and others, Chap. BD). Others are too short to intersect any of the seismic reflection profiles. Still others intersect the seismic profiles but do not always produce obvious offsets in reflectors. These would have to be interpreted as detachment faults that follow bedding planes for much of their length; they should be considered speculative until tested by a more thorough examination of the seismic data. The fault map suggests that most prospects within the Thin-Skinned Thrust-Belt Play (as mapped by Saltus and others, Chap. GR) are somewhat faulted, and some are severely faulted. This raises questions about the integrity of the trap seal for these prospects.

CONCLUSIONS

High-sensitivity aeromagnetic data over the ANWR 1002 area contain both low-amplitude, narrow linear anomalies produced by structurally deformed magnetitized layers near the top of the sedimentary section and high-amplitude, broad anomalies produced within the Franklinian basement. Matched-filtering has been successful in separating the anomalies produced by these two source regions.

Magnetic basement depths estimated from the lowpass (basement) magnetic field are largely consistent with basement and intra-basement depths as estimated from the seismic reflection profiles. The magnetic depth estimates consistently fall above the seismic basement surface in two areas, over the Hula-Hula Low and over the Demarcation Basin. In these two areas magnetic sources in the deeper sedimentary section may be masking any (weak) magnetic effect of the basement. This raises the possibility that further interpretation of the lowpass aeromagnetic data, along with the seismic reflection data, may reveal new prospective structures within the deeper parts of the Thin Skinned Thrust-Belt Play.

Magnetic models, based on combined highpass and bandpass aeromagnetic anomalies along three seismic reflection profiles, indicate that it is possible to reproduce the observed magnetic anomalies using folded and faulted normal and reversely magnetized layers that are coincident with layering seen in the seismic profiles. Such models provide tests of the structural and stratigraphic interpretations of the seismic profiles, and extend these interpretations into the shallowest part of the section (above the base of the permafrost layer).

Shallow faults can be mapped based on truncations of linear anomalies in the highpass aeromagnetic data. We know from the seismic profiles and surface geology that the Thin-Skinned Thrust-Belt Play is a highly faulted domain. The fault map prepared from the aeromagnetic data is useful for suggesting how shallow faults are connected between the seismic lines, and how short faults and detachment faults are distributed. The full extent of shallow faulting as revealed by the aeromagnetic interpretation suggests a reduction in the integrity of trap seals for prospects within this play.

REFERENCES

- Bird, K.J., and Molenaar, C.M., 1987, Stratigraphy: *in* Bird, K.J., and Magoon, L.B., eds., Petroleum geology of the northern part of the Arctic National Wildlife Refuge, northeastern Alaska, U.S. Geological Survey Bulletin 1778, p. 37-59.
- Brewer, M.C., 1987, Surficial geology, permafrost, and physical processes: *in* Bird, K.J., and Magoon, L.B., eds., Petroleum geology of the northern part of the Arctic National Wildlife Refuge, northeastern Alaska, U.S. Geological Survey Bulletin 1778, p. 27-36.
- Foland, R.L., and Lalla, D.J., 1987, Seismic-reflection data aquisition, processing, and interpretation: *in* Bird, K.J., and Magoon, L.B., eds., Petroleum geology of the northern part of the Arctic National Wildlife Refuge, northeastern Alaska, U.S. Geological Survey Bulletin 1778, p. 235-243.
- Molenaar, C.M., 1987, Introduction: *in* Bird, K.J., and Magoon, L.B., eds., Petroleum geology of the northern part of the Arctic National Wildlife Refuge, northeastern Alaska, U.S. Geological Survey Bulletin 1778, p. 3-6.
- Phillips, J.D., 1997, Potential-field geophysical software for the PC, version 2.2: U.S. Geological Survey Open-File Report 97-725, 34 p.

- Phillips, J.D., Saltus, R.W., and Reynolds, R.L., in press, Sources of magnetic anomalies over a sedimentary basin preliminary results from the coastal plain of the Arctic National Wildlife Refuge, Alaska in Gibson, R.I., and Milligan, P.S., eds., *Geologic Applications of Gravity and Magnetics: Case Histories*: Society of Exploration Geophysicists and American Association of Petroleum Geologists.
- Roest, W.R., and Pilkington, Mark, 1993, Identifying remanent magnetization effects in magnetic data: Geophysics, v. 58, no. 5, p. 653-659.

Figure AM1 - Index map showing topography and sea surface (color image), approximate coastline (dark blue line), 1002 boundary (magenta line), limits of aeromagnetic coverage (dashed black line), profile locations (red lines), and well locations (circles).

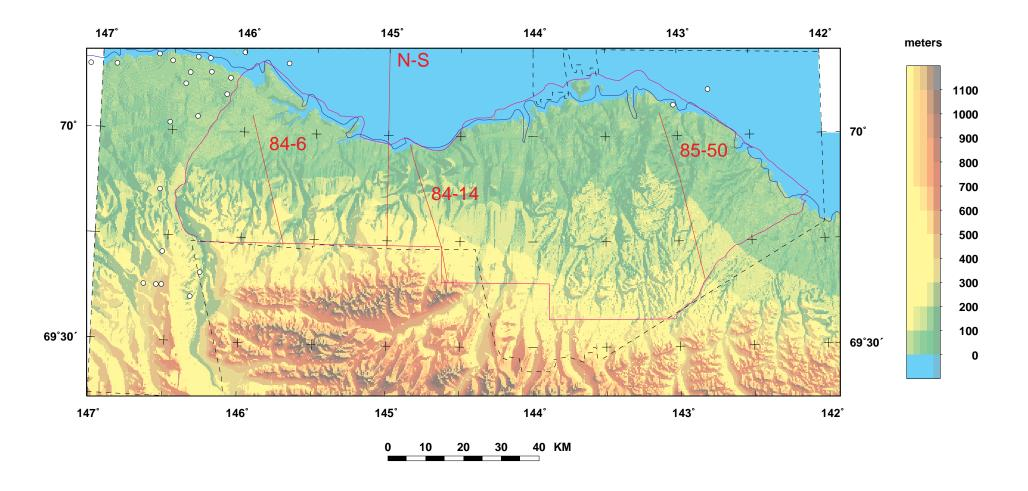


Figure AM2 - Power spectra of the aeromagnetic data (green) and of a model (red) consisting of three equivalent magnetic layers.

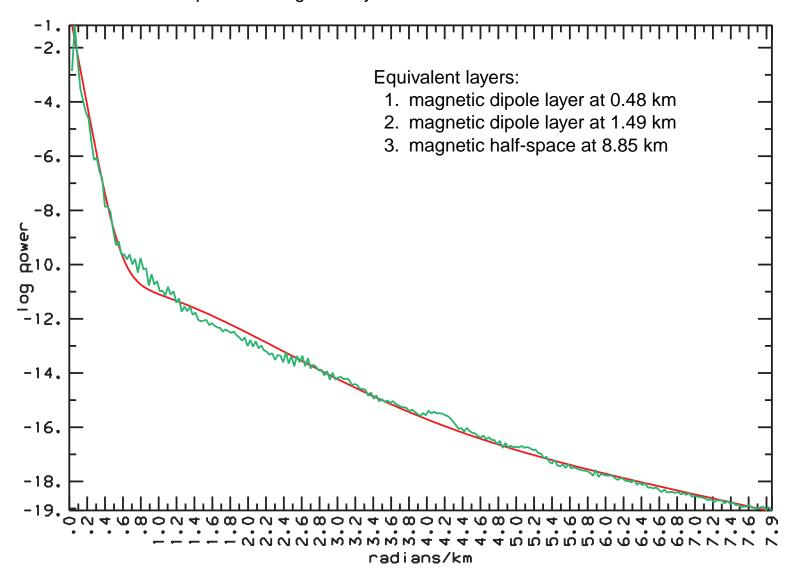


Figure AM3 - Bandpass filters corresponding to the three equivalent magnetic layers. Crossover wavelengths are indicated.

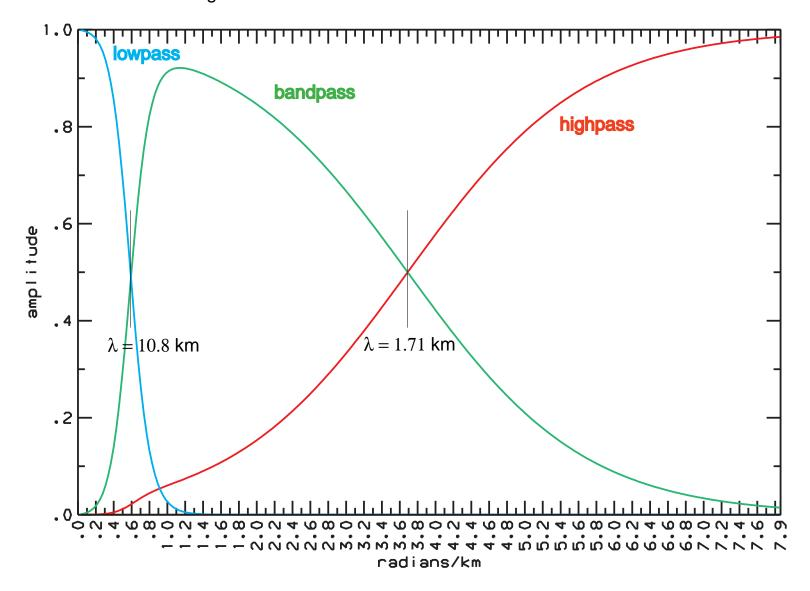


Figure AM4 - Results of bandpass filtering displayed along a north-south profile (profile NS, figure AM1).

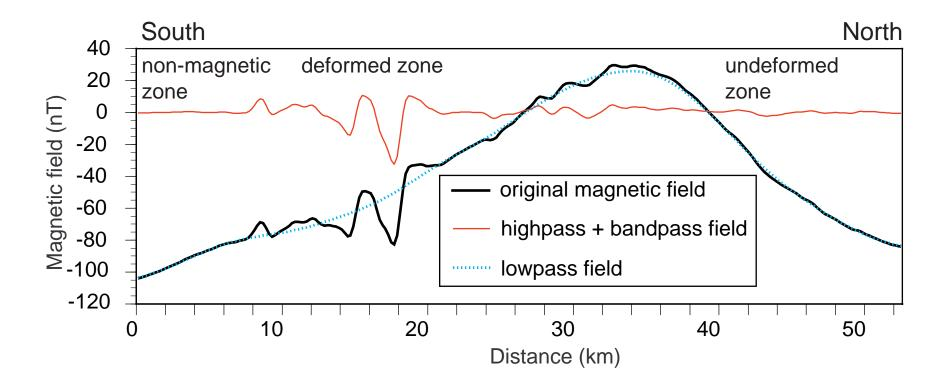


Figure AM5 - Lowpass magnetic field, showing magnetic anomalies produced largely within the Franklinian basement. The coastline is dark blue; the 1002 boundary is black.

Data is copyright BGM Airborne Surveys, Inc., a subsidiary of World Geoscience Corporation.

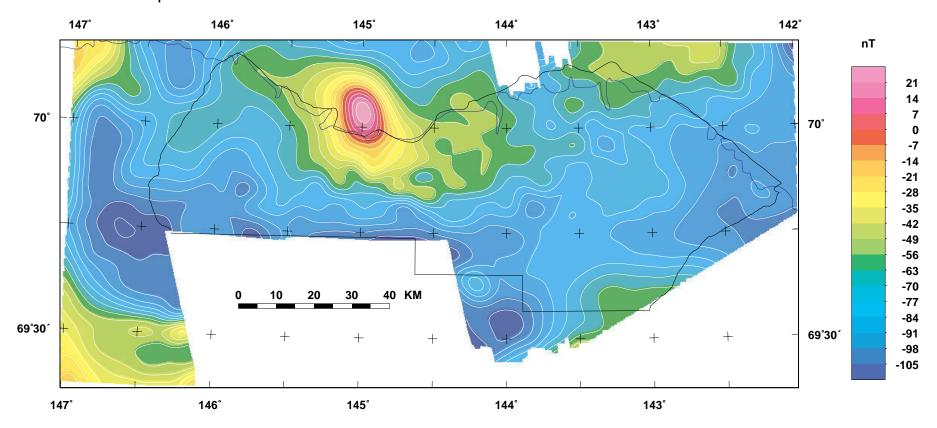


Figure AM6 - Minimum depth to magnetic basement as estimated from the lowpass magnetic field. White symbols indicate locations of depth estimates. These may line up along basement contacts or faults. Heavy hachured black lines indicate the intersection between this surface and the Top of the Pre-Mississippian (TPM, or seismic basement surface). The hachures point to areas where the magnetic basement surface falls below the TPM; elsewhere the magnetic basement surface lies above the TPM. The coastline is dark blue; the 1002 boundary is magenta.

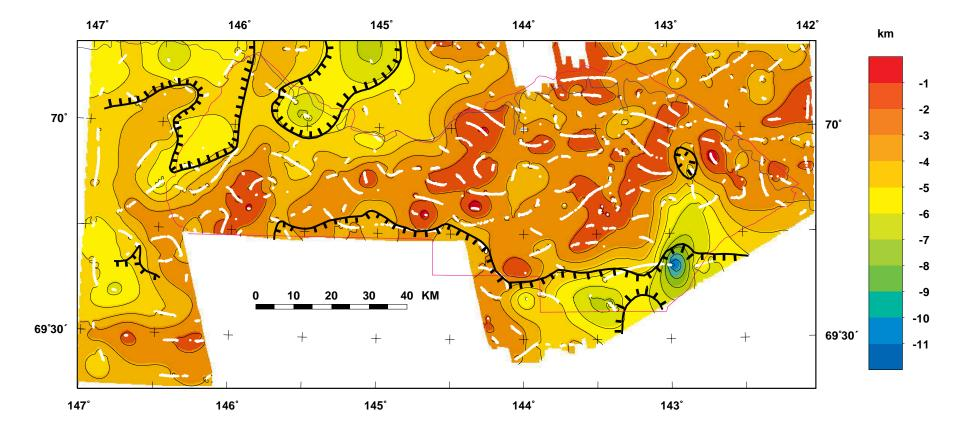


Figure AM7 - Maximum depth to magnetic basement as estimated from the lowpass magnetic field. White symbols indicate locations of depth estimates. Within the closed hachured heavy black line and east of the open hachured heavy black line, the magnetic basement surface lies above the Top of the Pre-Mississippian (TPM, or seismic basement) surface; elsewhere it lies below the TPM. The coastline is dark blue; the 1002 boundary is magenta.

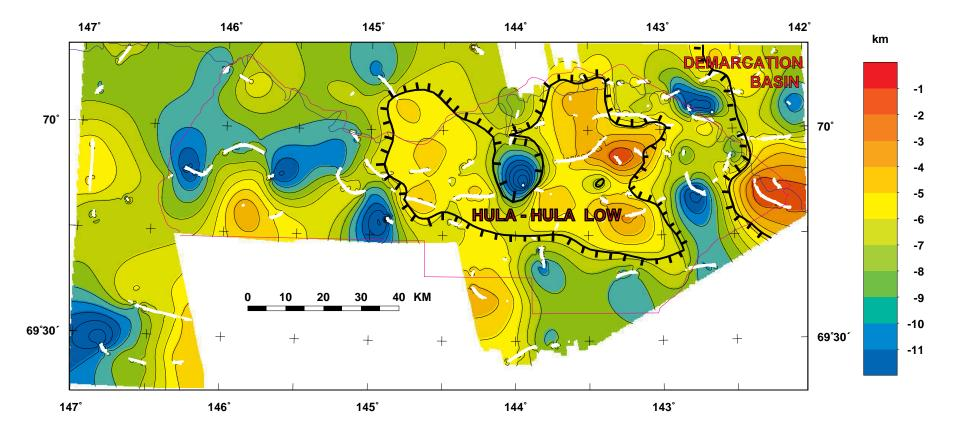


Figure AM8 - Magnetic model for the combined highpass and bandpass magnetic field along seismic profile 84-6.

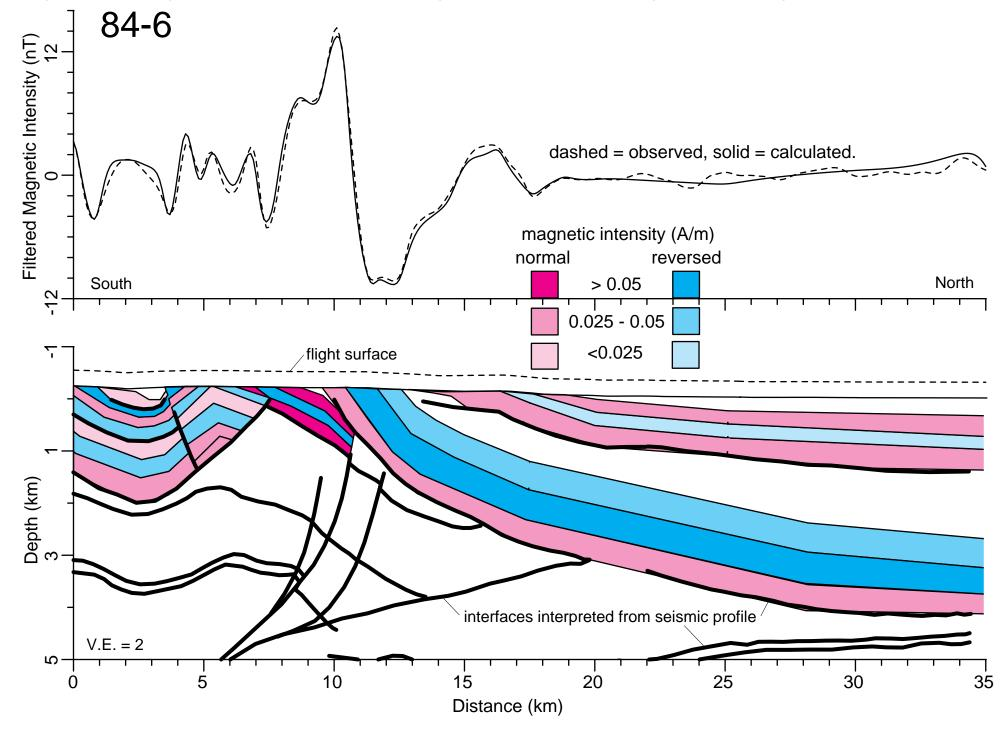


Figure AM9 - Magnetic model for the combined highpass and bandpass magnetic field along seismic profile 84-14.

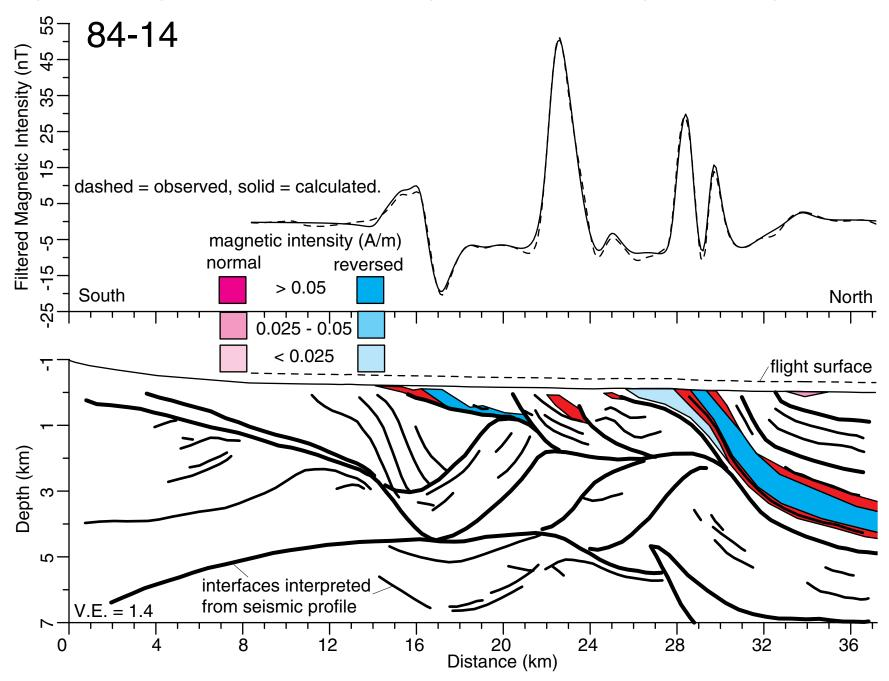


Figure AM10 - Magnetic model for the combined highpass and bandpass magnetic field along seismic profile 85-50.

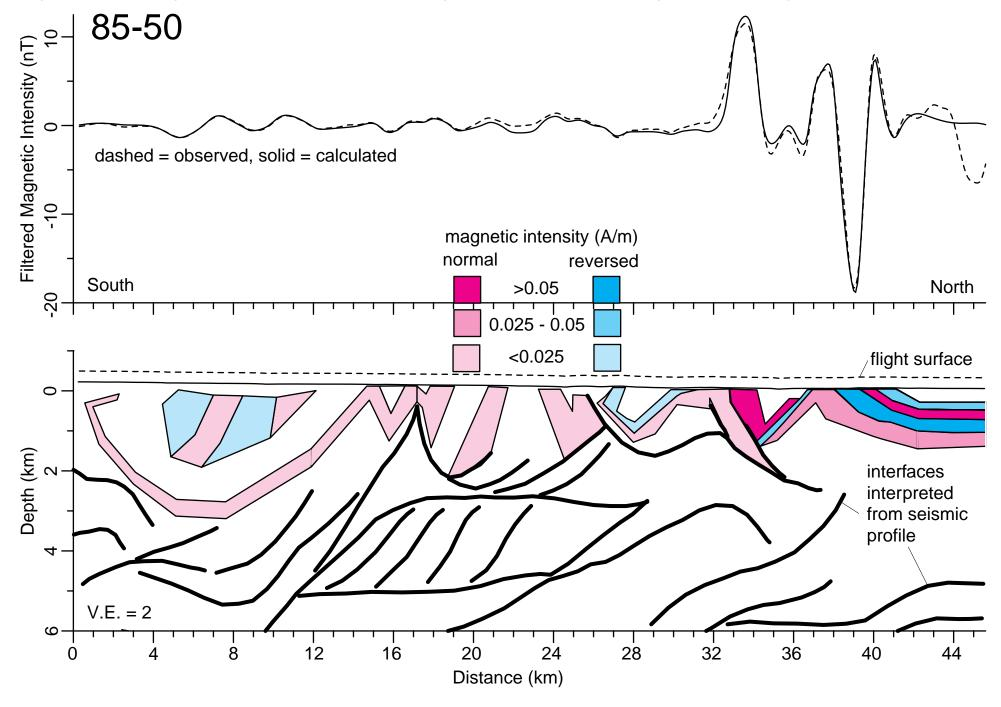


Figure AM11 - Near-surface fault map interpreted from the highpass aeromagnetic anomalies. The coastline is dark blue; the 1002 boundary is magenta.

